Article

Glial Cell Loss in the Anterior Cingulate Cortex, a Subregion of the Prefrontal Cortex, in Subjects With Schizophrenia

Anette K. Stark, M.D.

Harry B.M. Uylings, Prof., M.D., Ph.D.

Ernesto Sanz-Arigita, M.D., Ph.D.

Bente Pakkenberg, M.D., Dr.Med.Sci.

Objective: Structural deficits in the anterior cingulate cortex such as changes in glial cell and neuron numbers may be part of the anatomical substrate for schizophrenia and need to be investigated. The total number of neurons and glial cells in brains of 12 schizophrenia subjects and 14 comparison subjects were determined in two subdivisions of the prefrontal cortex: Brodmann's area 24, a part of the anterior cingulate cortex, and Brodmann's area 32 in the paracingulate cortex.

Method: The estimate of the total cell number was obtained by multiplying the volume of the region (estimated by using Cavalieri's point counting method) by the numerical density obtained from optical disectors in the cytoarchitectonically defined areas from the prefrontal cortex.

Results: The average total of bilateral glial cells in Brodmann's area 24 was 201×10^6 in subjects with schizophrenia and 302×10^6 in comparison subjects, a statistically significant difference of 33%, whereas there was a nonsignificant difference between the schizophrenia subjects and the comparison subjects in total number of glial cells in Brodmann's area 32. The bilateral average total number of neurons in areas 24 and 32 did not differ significantly between the schizophrenia and comparison subjects.

Conclusions: A selective reduction in glial cells in Brodmann's area 24 (but not in area 32) is seen in brains of subjects with schizophrenia relative to those of comparison subjects. Further investigations of the glial cells, their mutual relationship, and their relationship with neurons are needed to understand the role of specific glial components in this mental disorder.

(Am J Psychiatry 2004; 161:882–888)

Schizophrenia has been associated with several cortical structural abnormalities. Specifically, ventricular enlargement (1), reduced cortical volume (2, 3), and structural abnormalities of the frontal cortex have been reported repeatedly (for a review, see Lewis and Jeffrey [4]).

Because of its role in limbic functions, its significant dopaminergic innervation, and its role in development of human personality, we hypothesized that abnormalities in the prefrontal cortex (in particular the anterior cingulate cortex) might contribute to the pathology of schizophrenia. The anterior cingulate cortex has connections to both cortical and subcortical structures such as other parts of the prefrontal cortex, amygdala, thalamus, and the inferior parietal lobe. These connections enable the anterior cingulate cortex to bridge between the limbic structures and the frontal lobe and provide it with the capacity to integrate cognitive activity with affective experience (5–7).

Clinical studies of the anterior cingulate cortex in schizophrenia patients have reported abnormalities, including changed dopaminergic modulation during cognitive activity (8), reduction in blood flow and metabolism weeks after neuroleptic withdrawal (9, 10), and dysfunction and selective attention deficits during single-trial Stroop task in PET studies (11). Abnormalities of the prefrontal cortex and especially the anterior cingulate cortex described in schizophrenia are consistent with the known functions of this cortical region in information processing, attention, and in the expression and modulation of emotion (12, 13). Neuropathological studies have reported decreased neuronal density, abnormal spatial arrangement of neurons, and increased numbers of vertical association axons in the cingulate cortex of subjects with schizophrenia (14). Benes et al. (15) found the density of nonpyramidal neurons to be reduced by 16.2% in layer II of subjects with schizophrenia, with no difference in layers III through VI and no glial cell differences. Others have reported a reduction in glial cell density by 15%–20% and a neuronal volume reduction of 10%–15% in the anterior cingulate cortex of subjects with schizophrenia (16, 17). A specific astroglial reduction has been located in the dorsolateral prefrontal cortex (18). (For a review of microscopic neuropathology of schizophrenia, see Harrison [19].)

Glial cells have been implicated in a broad variety of functions (20), including cellular substrate for migration during CNS development (21), ion homeostasis (22), uptake of neurotransmitters (23), and contribution to the CNS immune system and neuromodulation (24).

TABLE 1. Clinical Characteristics of Schizophrenia and Comparison Subjects in a Study of Anterior Cingulate Cortex Structure

Group	Age (years)	Sex	Body Height (cm)	Body Weight (kg)	Age at First Admission (years)	Duration of Psychiatric Hospitalization (years)	Subdiagnosis	Duration of Neuroleptic Treatment (years)
Schizophrenia subjects								
1	85	F	170	58	46	49	Hebephrenic/catatonic	39
2	62	M	164	51	33	1–2	Paranoid	29
3	30	M	178	70	26	<1	Simple	5
4	56	M	170	81	39	2–3	Paranoid	13
5	56	M	174	90	50	3–4	Paranoid	>8
6	74	F	158	52	52	2–3	Paranoid	22
7	78	M	178	70	—	—	—	15
8	79	F	170	98	35	43	Residual	>12
9	80	F	160	61	31	1–2	Paranoid	—
10	85	F	165	50	45	1–2	Paranoid	19
11	76	M	172	74	26	50	Residual	—
12	75	M	—	55	21	55	—	>19
Mean	70		169	68	37	19		
SD	16		7	16	10			
Comparison subjects								
1	34	M	181	79				
2	55	M	174	77				
3	57	M	180	92				
4	65	M	173	85				
5	64	F	154	50				
6	71	M	175	78				
7	78	M	156	53				
8	80	F	162	47				
9	81	F	157	51				
10	85	F	159	39				
11	70	F	169	54				
12	75	F	172	56				
13	62	M	177	73				
14	83	F	160	71				
Mean	69		168	65				
SD	14		9	16				

For this study, we compared total cell numbers in two limbic prefrontal cortex subregions: Brodmann's area 24, a part of the anterior cingulate cortex, and Brodmann's area 32, a transitional region between the ventral agranular cingulate and the dorsal granular neocortex areas. Nissl staining is useful for counting neurons and glial cells, but it is not optimal for subpopulations of glial cells, wherefore subsampling was not performed. To our knowledge, this is the first report of glial cell quantification in Brodmann's area 32 in patients with schizophrenia.

Method

Subjects

The brains from the comparison subjects were part of another repository collected from 1987 to 1991 from autopsied individuals following the Danish laws on autopsied human tissue. The Danish ethical committee for Copenhagen and Frederiksberg approved the study. Table 1 shows demographic and clinical data for the schizophrenia and comparison subjects, and Table 2 shows postmortem data. No brains had evidence of degenerative brain disorders. The comparison brains came from 14 individuals who were free of neurological or psychiatric disorders. None of the subjects with schizophrenia or the comparison subjects had any history of head injury or substance abuse. The schizophrenia subjects fulfilled DSM-III criteria and belonged to a subpopulation of severely ill patients hospitalized for a substantial part of their lives and treated with neuroleptic treatment, insulin comas, or ECT. Furthermore, for both groups information about the patient's prehospital life was obtained from either close relatives or the general practitioner, thus excluding all patients with any CNS symptoms. The tissue was fixed within 8–72 hours after death and kept in 4% formaldehyde buffered with phosphate.

Tissue Processing

The meninges were removed from the brains, the right or left hemisphere chosen according to level of artifacts, and the hemispheres cut frontally into slabs that were 2.5 cm thick. The slabs were dehydrated in a series of alcohol solutions of 50%, 70%, and 80% (12 hours in each) and in 99% alcohol, xylene, and regular paraffin solutions (24 hours in each). The paraffin-embedded slabs were sectioned exhaustively into 40-µm-thick sections and were then systematically subsampled at random, providing about 10 sections per case (ranging from 9 to 15) containing Brodmann's area 24 and 32. These were adhered on object glasses pretreated with a gamma-aminopropyl-trithoxysilane and stained with a modified Giemsa stain (25).

Cytoarchitectonic Delineation

Brodmann's areas 24 and 32 were delineated by two independent investigators on coded slides, according to the cytoarchitectonic criteria specified in the following section. The interrater reliability of delineations was 95%–98%. An example of the transitional zone between areas 24 and 32 is shown in Figure 1.

Brodmann's area 24 occupies practically the entire extension of the cingulate gyrus, stretching from the adjacent area 33 to its dorsal limit. The lack of granular layer IV and the salience of the pyramidal layer V are characteristic features of the region (26). Layer V is composed of a population of well-stained big pyramids

TABLE 2. Postmortem Data of Schizophrenia and Comparison Subjects in a Study of Anterior Cingulate Cortex Structure

Group	Cause of Death	Brain Weight (g)	Terminal Period (days)	Postmortem Interval (hours)	Fixation Period (years)	Hemisphere Sampled
Schizophrenia subjects						
1	Pneumonia	1100	18	45	12	Right
2	Acute myocardial infarction	1160	0.1	24	14	Left
3	Suicide	1420	0.1	60	7.5	Right
4	Bronchitis	1320	3	72	10.5	Right
5	Acute myocardial infarction	1470	2	24	13	Left
6	Colon cancer	1220	3	24	3	Right
7	Acute myocardial infarction	1260	0.1	20	15	Right
8	Sepsis; diabetes mellitus	1198	7	36	2.5	Left
9	Breast cancer	1100	18	48	10.5	Right
10	Acute myocardial infarction	1070	0.1	23.5	4	Left
11	Acute myocardial infarction	1320	0.1	21	25	Left
12	Acute myocardial infarction	860	3	29	25	Right
Mean		1208		35.5	9.5	
SD		167		17	7.5	
Comparison subjects						
1	Bleeding, homicide	1230	0.2	8	9	Left
2	Acute myocardial infarction	1160	6	72	8	Left
3	Acute myocardial infarction	1390	0.1	24	6	Left
4	Acute myocardial infarction	1420	0.1	24	5.5	Right
5	Acute myocardial infarction	1240	0.1	24	7.5	Right
6	Acute myocardial infarction	1380	0.1	48	1	Right
7	Aorta aneurysm	1200	0.1	48	6	Left
8	Congestive heart failure	970	0	12	8	Left
9	Acute myocardial infarction	1090	7	24	8	Left
10	Acute myocardial infarction	1180	14	24	11	Right
11	Acute myocardial infarction	1334	0.1	33	8	Right
12	Congestive heart failure	1138	0.1	35	8	Left
13	Acute myocardial infarction	1460	0.1	28.5	12	Left
14	Acute myocardial infarction	1080	0.1	24	21	Left
Mean		1233		30.6	8.5	
SD		145		16	4.4	

distributed in two levels: the upper sublayer Va, with a homogeneous distribution and high cell density in contrast to the underlying sublayer Vb, characterized by pyramids aggregating into distinct cellular clusters with an overall low cellular density and the presence (often in clusters) of spindle (fusiform) neurons (27, 28). These attributes influence the global aspect of its structural pattern, giving it a bistratified appearance clearly visible already at low magnification. The overall bilaminar aspect and the absence of layer IV help to differentiate area 24 from the neighboring dorsal and rostral areas. Ventral to the corpus callosum, the entire region shares the bilaminar layout in the lower layers described for area 24. Here the granularity criterion prevails, offering a reliable reference to the limit between the agranular area 24 and the granular Brodmann's area 12.

Brodmann's area 32 can be considered as a transitional region between peri- and isocortex and has been roughly associated to the paracingulate gyrus, also called the superior cingulate or paracingulate cortex. In this case, however, the relationship between microstructure and gross anatomical features proves to be unreliable, since the gyrus shows a high degree of morphological variability and is often fragmented. It is positioned basically parallel to the adjacent cingulate gyrus, connecting to the cingulate gyrus and the superior rostral sulcus at the level of the genu of the corpus callosum (29). The main properties of area 32 are the progressive predominance of supragranular layers II and III over the infragranular layers V and VI and the development of a discontinuous internal, granular layer IV. Area 32 is composed of pyramidal cells and shows a moderate but continuous increase in cell size from surface toward the white matter. Sublayer IIIc is particularly developed, and its cells intermingle with those belonging to the upper limit of the pyramidal layer V. Furthermore, layer V is more homogeneous than in area 24, with a diminishing sublayer Va, while simultaneously increasing cellular density and width of sublayer Vb. The appearance of layer IV and a wide layer III marks the ventral limit of area 32. Rostrally, area 32 is distinguishable from area 10 by the rich layer IV of the latter. The transition between the end of area 32 and the beginning of the supplementary motor area or cingulate magnoganglionic core of Braak (27, 30) is revealed by the sudden appearance of the pyramidal cells of Betz in layer Vb, a distinctive feature of motor cortices (31). No extension of area 32 ventral to the corpus callosum has been detected (31).

Stereology

A combination of systematic uniformly random sampling, volume estimation, cell counting, and disectors was used to obtain the total number of neurons and glial cells.

For systematic uniformly random sampling, some of the most remarkable features are the efficiency in terms of time and precision that may be obtained by counting only a few hundred nerve cells in, for example, the human brain. The coefficient of error (CE) of the estimated total cell number was determined according to the formula given by Braendgaard et al. (25) and modified according to equations 20–22 of Gundersen et al. (32). In the estimation of total cell number, we considered the "ideal" coefficient of error to be about half of the observed coefficient of variation (CV) because of the relationship: observed CV^2=biological CV^2 + estimator CE^2 (32). In this study, the values of the coefficient of variation were about 20%–30%, and the values of the coefficient of error were about 10%, which means that we met our general criteria for optimal precision of the estimations.

The total volume of the brain region of interest, i.e., the volume of the reference space [V(ref)] was estimated by using the Cavalieri principle (33). The total number of points [ΣP_i] is multiplied

FIGURE 1. Delineation of Brodmann's Areas 24 and 32 and the Transitional Zone[a]

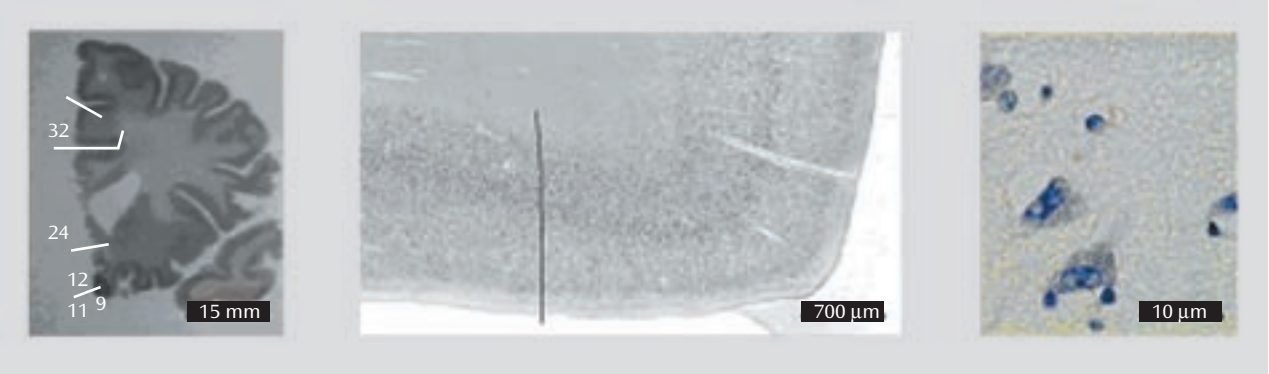

[a] An example of the transitional zone between 24 and 32 in low magnification (left). At higher magnification (middle), area 24 is shown adjacent to area 32 with region 24 to the left of region 32. Examples of typical neuron and glial cells (right). Scale bars indicate level of magnification.

by the unit area per point [a(p)] to give the total area of interest: $A_i=a(p)\times\Sigma P$. The area [A_i] of each region was estimated using a Leica DMLB microscope with a 2.5× objective and a final magnification of 172× and an area per point of 1517 mm^2. A camera lucida setup was used to superimpose the cross-sectional area of the region of interest onto a point counting grid, and the investigator counted only the points that were within the image of the area. The average number of points counted per brain was 122 (range=90–208) for area 24 and 87 (range=32–187) for area 32.

The third dimension of the reference volume [V(ref)] was obtained by multiplying the sum of the measured areas [ΣA_i] by the inverse sampling frequency of the sections [k] and the section thickness [t]: $V(ref)=\Sigma A_i\times k\times t$.

The cell counting was performed by using the optical disector method to estimate the number of cells divided into two groups (neurons and glial cells) in Brodmann's areas 24 and 32. Bilateral cell number was estimated as the unilateral number multiplied by two.

The disector is a probe that samples isolated particles with a uniform probability in three-dimensional space in which the z axis (the height of the disector) is employed using 40-µm-thick sections in which the plane of focus is moved up or down, and the x and y axis are defined by a square (the counting frame) superimposed on the magnified image of the tissue on the computer screen (34). The area of the counting frame [a(frame)], the height of the disector [h], and the sampling fraction in the x-y axis were estimated in a pilot study and optimized to obtain a count of approximately 150–200 particles (cells) [ΣQ^-] per specimen. The dimension of the optical disector probe was a rectangular frame area of 2171 μm^2 and a disector height of 20 µm. The volume of the disector [v(dis)] is calculated as follows: $v(dis)=h\times a(frame)$. The equipment for optical disector counting consisted of a BX-50 Olympus microscope with a 100× oil-immersion objective with a high numerical aperture (1.35), a motorized stage, and an electronic Heidenhain microcator with a digital readout for measuring movements in the z direction with a precision of 0.5 µm. Counting took place at a final magnification of 3250×. Per brain, an average of 105 disector probes (range=32–208) were sampled with an average number of 1.5 neurons (range=0.9–2.8) and 3.0 glial cells (range=0.5–5.1) counted per disector, respectively. The thickness of the stained sections was measured at every second disector, showing a mean section thickness of 37.4 µm (range=31.9–45.3). The distinction between the largest glial cells and the smallest neurons is not a trivial problem. In this study, the neurons were identified on a combination of morphological criteria such as the chromatin pattern, size, and shape of the cell nucleus, a clearly visible nucleolus, and surrounding cytoplasm. Figure 1 shows examples of neuron and glial cells using the modified Giemsa stain applied in this study. In 1.3% of the cases, the cells were identified as nonclassifiable and were not included in the final estimate. One investigator (A.K.S.) performed all cell counting. Several brains were counted more than once in a coded design and showed an intrarater reliability of >95% in total cell number.

The total number of particles (cells) [N(part)] was obtained from the equation $N(part)=[\Sigma Q^-/\Sigma v(dis)]\times V(ref)$, where $\Sigma Q^-/\Sigma v(dis)$ is equal to the numerical cell density [N_v]. Since the estimation of both the numerical cell density and the reference volume was obtained at the final, processed histological tissue level, the shrinkage does not need to be calibrated.

Statistical Analyses

The differences between means were analyzed using an unpaired two-tailed Student's t test. The p values of differences between means are presented as two-tailed probabilities. Variability is shown in brackets as coefficient of variability (CV=SD/mean) following the respective means.

Results

As seen in Figure 2, the mean total number of neurons in the bilateral Brodmann's area 24 was 130×10^6 (CV=0.37) for subjects with schizophrenia and 138×10^6 (CV=0.26) for comparison subjects, a statistically nonsignificant difference of 5.66%. The mean total number of neurons in the bilateral Brodmann's area 32 was 86×10^6 (CV=0.38) for subjects with schizophrenia and 92×10^6 (CV=0.28) for comparison subjects, a statistically nonsignificant difference of 6.65%. For this study more left hemispheres than right hemispheres were included, but in accordance with earlier studies we found no difference in total number of neurons between the two hemispheres in either Brodmann's area 24 or 32 (e.g., the mean total number of neurons in area 24 hemispheres was 137×10^6 for the right and 132×10^6 for the left, a statistically nonsignificant difference of 2.46% [t=0.30, df=24, p=0.77]).

As seen in Figure 3, the mean total number of glial cells in the bilateral Brodmann's area 24 was significantly less in

FIGURE 2. Total Number of Neurons in Brodmann's Areas 24 and 32 in Schizophrenia and Comparison Subjects

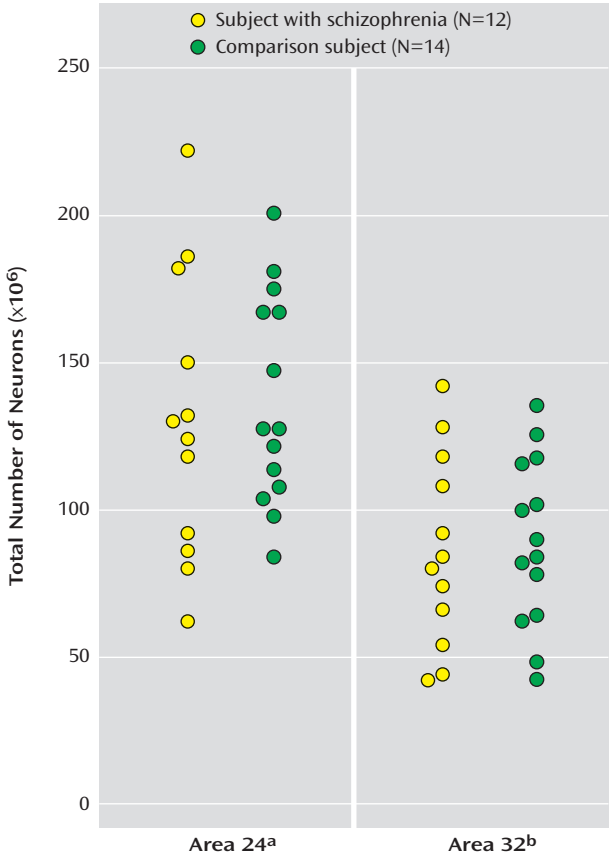

[a] Nonsignificant between-group difference (F=–0.47, df=1, 24, p=0.64).
[b] Nonsignificant between-group difference (F=–0.53, df=1, 24, p=0.60).

FIGURE 3. Total Number of Glial Cells in Brodmann's Areas 24 and 32 in Schizophrenia and Comparison Subjects

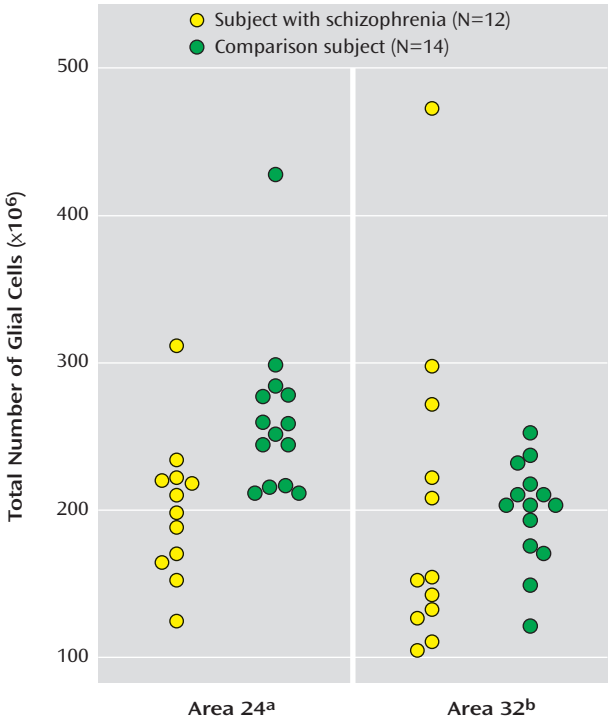

[a] Significant between-group difference (F=–2.94, df=1, 24, p=0.007).
[b] Nonsignificant between-group difference (F=–0.79, df=1, 24, p=0.44).

subjects with schizophrenia (201×10^6 [CV=0.24]) than in comparison subjects (302×10^6 [CV=0.36]), a significant difference of 33.43%. The mean total number of glial cells in the bilateral Brodmann's area 32 was 164×10^6 (CV=0.44) for subjects with schizophrenia and 186×10^6 (CV=0.37) for comparison subjects, a nonsignificant difference of 11.8%.

No statistically significant difference was found between the average neuron or glial cell densities in Brodmann's areas 24 and 32 of subjects with schizophrenia and comparison subjects. However, the difference in glial cell density in Brodmann's area 24 between subjects with schizophrenia ($57\times10^3/mm^3$ [CV=0.29]) and comparison subjects ($70\times10^3/mm^3$ [CV=0.27]) approached significance ($p<0.08$). The glial density in area 32 was $63\times10^3/mm^3$ for schizophrenia subjects and $66\times10^3/mm^3$ for comparison subjects. Neuron density in area 24 was $130\times10^3/mm^3$ for schizophrenia subjects and $138\times10^3/mm^3$ for comparison subjects. Neuron density in area 32 was $33\times10^3/mm^3$ for both groups. These density values are uncorrected for histological shrinkage.

No significant differences in total bilateral volume were found. The mean total bilateral volume of Brodmann's area 24 was 3.8×10^3 mm^3 and 4.2×10^3 mm^3 for subjects with schizophrenia and comparison subjects, respectively (t=–1.17, df=24, p=0.25). The mean total bilateral volume of Brodmann's area 32 was 2.6×10^3 mm^3 and 2.8×10^3 mm^3 for subjects with schizophrenia and comparison subjects, respectively (t=–0.65, df=24, p=0.52).

There was no correlation between total number of cells and fixation period and no correlations for total cell number, glial cells, or neurons in Brodmann's areas 24 and 32 with postmortem interval or neuroleptic treatment, which is in agreement with the literature indicating that pharmacological treatments are more likely to increase glial cell numbers than to cause a reduction (35).

Discussion

This study demonstrates that the total number of glial cells in the bilateral Brodmann's area 24 was significantly lower in subjects with schizophrenia relative to comparison subjects, with no change in total neuron numbers. Our results differ from previous neuronal counting studies that reported postmortem reduction in neuron density in Brodmann's area 24 of subjects with schizophrenia (13, 14, 36), but are in agreement with our normal neuron numbers in the prefrontal cortex (37) and frontal lobes (38). Brodmann's area 32 is structurally defined as a "transitional" area, sharing structural features with the bordering periallocortical area 24 and fully isocortical regions. De-

spite its related structural properties, area 32 is spared of the reduction of glial cells found in area 24, indicating a particular involvement of Brodmann's area 24 in the structural changes associated with schizophrenia.

We did not find any differences in the cell densities of either neurons or glial cells, although the glial cell density in Brodmann's area 24 was close to being significantly reduced in the subjects with schizophrenia relative to the comparison subjects. However, as stressed previously (37), alterations in cell density do not necessarily reflect alterations in the total cell number. Differences in cell densities can simply signify differences in tissue behavior (shrinkage or swelling) during histological handling, with an unpredictable impact on the cell density.

Because glial cells are suspected of playing an essential role in normal brain functioning, we believe that it is significant that our study identified a schizophrenia-associated deficit in total number of glial cells in the anterior cingulate cortex. Oligodendrocytes, the myelin-forming cells of the central nervous system, and astrocytes constitute macroglia, which are able to respond to changes in the cellular and extracellular environment. Despite their number and their role during development, their active participation in the physiology of the brain and the consequences of their dysfunction on the pathology of the CNS have only been emphasized in recent years (20). Using gold impregnation, Ramon y Cajal (39) identified the astrocyte, while Rio Hortega a few years later identified the oligodendrocyte, and another cell type that he distinguished from the two macroglial cells as the microglia (40). There is now increasing evidence that glia, possibly through a glial network, may have communication skills that complement those of the neurons themselves (20).

Using recent stereological methods, the role of glial cells in the prefrontal cortex of schizophrenia has been investigated in a few studies. Öngür et al. (41) found glial cell reductions in spite of normal neuron numbers in selected areas of the prefrontal cortex (the subgenual part of Brodmann's area 24) in mood disorders but with no changes of neuronal and glial cell numbers in schizophrenia brains studied as psychiatric control subjects, while Pierri et al. (42) found reduced mean neuronal size in deep layer III pyramidal neurons in schizophrenia subjects relative to comparison subjects. In our study, the glial cells were not subdivided into subgroups. It would thus be premature to postulate mechanisms leading from total glial reduction to the psychopathology of schizophrenia. The role of glial cell reduction in the prefrontal cortex is uncertain in the pathogenesis of schizophrenia, but the reduction presumably interacts with other factors, including afferent neuronal activity or neuromodulators such as serotonin, noradrenalin, and dopamine to produce specific disturbances in brain activity, mood, and behavior. It is possible that glial cell loss could predate or predispose to schizophrenia, and it is of course also possible that glial cell loss could be an epiphenomenon and thus not of primary etiological importance to the disease process.

Future studies of clinicopathological correlates and of the effects of drug therapy on glial cells and glial-neuronal relationships may verify the role of glial cell pathology in schizophrenia.

Presented in part at the 31st annual meeting of the Society for Neuroscience, San Diego, November 10–15, 2001. Received Nov. 14, 2002; revision received Sept. 2, 2003; accepted Sept. 5, 2003. From the Research Laboratory for Stereology and Neuroscience, Bispebjerg Hospital; the Netherlands Institute for Brain Research, Royal Netherlands Academy of Arts and Sciences, Amsterdam; and the Department of Anatomy, Vrije Universiteit Medical Center, Graduate School Neurosciences Amsterdam, the Netherlands. Address reprint requests to Dr. Stark, Research Laboratory for Stereology and Neuroscience, Bispebjerg Hospital, Bispebjerg Bakke, 2400 Copenhagen NV, Denmark; forsklab@bbh.hosp.dk (e-mail).

Supported by a scholarship provided by the Copenhagen Hospital Corporation Research Council, H:S; and by funding from the Hartmann Brothers' Foundation and the Lily Benthine Lund's Foundation.

The authors thank Risskov Psychiatric Hospital for providing part of the tissue.

References

1. Johnstone EC, Crow TJ, Frith CD, Husband J, Kreel L: Cerebral ventricular size and cognitive impairment in chronic schizophrenia. Lancet 1976; 2:924–926
2. Wright IC, Rabe-Hesketh S, Woodruff PWR, David AS, Murray RM, Bullmore ET: Meta-analysis of regional brain volumes in schizophrenia. Am J Psychiatry 2000; 157:16–25
3. Hulshoff Pol HE, Schnack HG, Bertens MGBC, van Haren NEM, van der Tweel I, Staal WG, Baaré WFC, Kahn RS: Volume changes in gray matter in patients with schizophrenia. Am J Psychiatry 2002; 159:244–250
4. Lewis DA, Jeffrey AL: Catching up on schizophrenia: natural history and neurobiology. Neuron 2000; 28:325–334
5. Groenewegen HJ, Uylings HBM: The prefrontal cortex and the integration of sensory, limbic and autonomic information. Prog Brain Res 2000; 126:3–28
6. Zilles K: Cortex, in The Human Nervous System. Edited by Paxinos G. San Diego, Academic Press, 1990, pp 757–802
7. Vogt BA, Vogt LJ, Nimchinsky EA, Hof PR: Primate cingulate cortex chemoarchitecture and its disruption in Alzheimer's disease, in Handbook of Chemical Neuroanatomy vol 13: The Nervous System. Edited by Bloom FE, Björklund A, Hökfelt T. Amsterdam, Elsevier 1997, pp 455–528
8. Dolan RJ, Fletcher P, Frith CD, Friston KJ, Frackowiak RSJ, Grasby PM: Dopaminergic modulation of impaired cognitive activation in the anterior cingulate cortex in schizophrenia. Nature 1995; 378:180–182
9. Holcomb HH, Cascella NG, Thaker GK, Medoff DR, Dannals RF, Tamminga CA: Functional sites of neuroleptic drug action in the human brain: PET/FDG studies with and without haloperidol. Am J Psychiatry 1996; 153:41–49
10. Miller DD, Andreasen NC, O'Leary DS, Rezai K, Watkins GL, Boles Ponto LL, Hichwa RD: Effect of antipsychotics on regional cerebral blood flow measured with positron emission tomography. Neuropsychopharmacology 1997; 17:230–240; correction, 1998; 18:323–324
11. Carter CS, Mintun M, Nichols T, Cohen JD: Anterior cingulate gyrus dysfunction and selective attention deficits in schizophrenia: $[^{15}O]H_2O$ PET study during single-trial Stroop task performance. Am J Psychiatry 1997; 154:1670–1675

12. Fuster JM: The prefrontal cortex, in Anatomy, Physiology, and Neuropsychology of the Frontal Lobe. Philadelphia, Lippincott-Raven 1997, pp 172–176, 202–204
13. Posner MI, Petersen SE: The attention system of the human brain. Annu Rev Neurosci 1990; 13:25–42
14. Benes FM: Cortical pathology: a new generation of quantitative microscopic studies, in The Neuropathology of Schizophrenia. Edited by Harrison PJ, Roberts GW. Oxford, UK, Oxford University Press, 2001, pp 81–104
15. Benes FM, McSparren J, Bird ED, San Giovanni JP, Vincent SL: Deficits in small interneurons in prefrontal and cingulate cortices of schizophrenic and schizoaffective patients. Arch Gen Psychiatry 1991; 48:996–1001
16. Cotter DR, Pariante CM, Rajkowska G: Glial pathology and major psychiatric disorders, in The Postmortem Brain in Psychiatric Research. Edited by Agam G, Everall IP, Belmaker RH. Boston, Kluwer Academic, 2002, pp 49–73
17. Cotter D, Mackay D, Landau S, Kerwin R, Everall I: Reduced glial cell density and neuronal size in the anterior cingulate cortex in major depressive disorder. Arch Gen Psychiatry 2001; 58: 545–553
18. Rajkowska G, Miguel-Hidalgo JJ, Makkos Z, Meltzer H, Overholser J, Stockmeier C: Layer-specific reductions in GFAP-reactive astroglia in the dorsolateral prefrontal cortex in schizophrenia. Schizophr Res 2002; 57:127–138; correction, 2003; 60:103
19. Harrison PJ: The neuropathology of schizophrenia: a critical review of the data and their interpretation. Brain 1999; 122:593–624
20. Baumann N, Pham-Dinh D: Biology of oligodendrocyte and myelin in the mammalian central nervous system. Physiol Rev 2001; 81:871–927
21. Rakic P: A small step for the cell, a giant leap for mankind: a hypothesis of neocortical expansion during evolution. Trends Neurosci 1995; 18:383–388
22. Tsacopoulos M, Magistretti PJ: Metabolic coupling between glia and neurons. J Neurosci 1996; 16:877–885
23. Henn F: Neurotransmitters and astroglia lead to neuromodulation. Prog Brain Res 1982; 55:241–252
24. Barres BA, Barde Y: Neuronal and glial cell biology. Curr Opin Neurobiol 2000; 10:642–648
25. Braendgaard H, Evans SM, Howard CV, Gundersen HJG: The total number of neurons in the human neocortex unbiasedly estimated using optical disectors. J Microsc 1990; 157:285–304
26. Vogt BA, Nimchinsky EA, Vogt LJ, Hof PR: Human cingulate cortex: surface features, flat maps, and cytoarchitecture. J Comp Neurol 1995; 359:490–506
27. Braak H: Architectonics of the Human Telencephalic Cortex. Berlin, Springer Verlag, 1980
28. Nimchinsky EA, Vogt BA, Morrison JH, Hof PR: Spindle neurons of the human anterior cingulate cortex. J Comp Neurol 1995; 355:27–37
29. Paus T, Tomaiuolo F, Otaky N, MacDonald D, Petrides M, Atlas J, Morris R, Evans AC: Human cingulate and paracingulate sulci: pattern, variability, asymmetry, and probabilistic map. Cereb Cortex 1996; 6:207–214
30. Braak H, Braak E: The pyramidal cells of Betz within the cingulate and precentral gigantopyramidal field in the human brain: a Golgi and pigment architectonic study. Cell Tissue Res 1976; 172:103–119
31. Sanz-Arigita E, De Vos K, Pool CW, Zilles K, Uylings HBM: 3-D cytoarchitectonic probabilistic map of human medial prefrontal cortex. Neuroimage 2001; 13:S236
32. Gundersen HJG, Jensen EBV, Kieu K, Nielsen J: The efficiency of systematic sampling in stereology—reconsidered. J Microsc 1999; 193:199–211
33. Gundersen HJG, Jensen EB: The efficiency of systematic sampling in stereology and its prediction. J Microsc 1987; 147:229–263
34. Sterio DC: The unbiased estimation of number and sizes of arbitrary particles using the disector. J Microsc 1984; 134:127–136
35. Selemon LD, Rajkowska G, Goldman-Rakic PS: Increased volume and glial density in primate prefrontal cortex associated with chronic antipsychotic drug exposure. Biol Psychiatry 1999; 46:161–172
36. Chua SE, McKenna PJ: A skeptical view of the neuropathology of schizophrenia, in The Neuropathology of Schizophrenia: Progress and Interpretation. Edited by Harrison PJ, Roberts GW. Oxford, UK, Oxford University Press, 2001, pp 291–337
37. Thune JJ, Uylings HBM, Pakkenberg B: No deficit in total number of neurons in the prefrontal cortex in schizophrenics. J Psychiatr Res 2001; 35:15–21
38. Pakkenberg B: Total nerve cell number in neocortex in chronic schizophrenics and controls estimated using optical disectors. Biol Psychiatry 1993; 34:768–772
39. Ramon y Cajal S: Contribucion al concimiento de la neurologia del cerebro humano. Trab Lab Inves Biol (Madrid) 1913; 11: 255–315
40. Rio Hortega DP: Tercera aportasion al conocimiento morfologico a interpretacion functional de la oligodendroglia. Memor Real Soc Esp Hist Nat 1928; 14:5–122
41. Öngür D, Drevets WC, Price JL: Glial reductions in the subgenual prefrontal cortex in mood disorders. Proc Natl Acad Sci USA 1998; 95:13290–13295
42. Pierri JN, Volk CLE, Auh S, Sampson A, Lewis DA: Decreased somal size of deep layer 3 pyramidal neurons in the prefrontal cortex of subjects with schizophrenia. Arch Gen Psychiatry 2001; 58:466–473